The power of help: mechanistic insights into CD4⁺ T cell differentiation in vaccination and cancer

Bosma, D.M.T.

Chapter 3

CD4$^+$ T-cell help delivery to monocyte-derived dendritic cells promotes effector differentiation of helper and cytotoxic T cells

Douwe M. T. Bosma[1], Julia Busselaar[1], Mo D. Staal[1], Elselien Frijlink[1], Matthias Mack[2], Fiamma Salerno[1,*] and Jannie Borst[1,*]

1 Department of Immunology, Leiden University Medical Center, Leiden, the Netherlands.

2 Department of Internal Medicine II, University Hospital Regensburg, Regensburg, Germany.

** Shared last authors*

Published in Immunology Letters. 2025; Oct:275:107022
Doi: 10.1016/j.imlet.2025.107022

Abstract

Delivery of $CD4^+$ T-cell help optimizes $CD8^+$ T-cell effector and memory responses via CD40-mediated licensing of conventional dendritic cells (DCs). Using comparative vaccination settings that prime $CD8^+$ T cells in presence or absence of $CD4^+$ T-cell help, we observed that $CD4^+$ T-cell activation promoted influx of monocytes into the vaccine-draining lymph nodes (dLNs), where they differentiated into monocyte-derived (Mo)DCs, as defined by the most recent standards. Abrogation of these responses by CCR2-targeted depletion indicated that monocyte-derived cells in the dLN promoted T-helper 1 (Th1) type effector differentiation of $CD4^+$ T cells, as well as clonal expansion and effector differentiation of $CD8^+$ T cells. Monocyte-derived cells in dLNs upregulated CD40, CD80 and PD-L1 as a result of $CD4^+$ T-cell help. The response of monocyte-derived cells to $CD4^+$ T-cell help was independent of natural killer (NK) cells and proceeded via CD40 ligand (L)-CD40 interactions and IFNγ signaling. Our data argue for a scenario wherein activated $CD4^+$ T cells in dLNs crosstalk via CD40L and IFNγ signals to monocytes, promoting their local differentiation into MoDCs. This event enhances formation of $CD4^+$ Th1 and $CD8^+$ cytotoxic effector T cell pool, most likely by virtue of their improved costimulatory status and cytokine production.

Keywords:

T-cell priming, Monocyte, MoDC, Vaccination, $CD4^+$ T-cell help

Introduction

Adaptive immune responses by T and B cells are critical for pathogen control and successful vaccination because they generate memory and long-term protection. T-cell priming depends on conventional (c)DCs that present antigen and, upon activation, deliver costimulatory signals and cytokines essential for activation, clonal expansion and effector differentiation of CD4+ and CD8+ T cells. Pre-cDCs enter peripheral tissues and secondary lymphoid organs at steady-state via the blood and there become competent migratory (m)cDC or LN-resident (r)cDC subsets respectively[1,2]. Generally, cDCs have optimal phagocytic capacities and scavenge their environment for soluble or cell-associated antigens. Migratory cDCs expressing the chemokine receptor CCR7 bring self-antigens derived from apoptotic cells at steady state to dLNs and thereby promote self-tolerance[3,4]. Apart from this, soluble antigens can passively drain to LNs via the lymphatics. At steady state, rcDCs and, in particular rcDC2s are localized near lymphatic sinuses[5], where they can rapidly sense draining antigens. RcDC1s are more homogeneously distributed throughout the T-cell zone where antigen delivery is limited[4]. The relative contribution of mcDCs versus rcDCs to T-cell priming depends on antigen load and location[6]. Upon infection, cancer, or vaccination, cDCs become activated by pathogen- or damage-associated molecular patterns (PAMPs or DAMPs). As a result, their migration to dLNs is intensified and foreign antigens are efficiently delivered for T-cell activation[3]. CD4+ T cells recognize antigens in the context of MHC class II (MHC-II) and are therefore geared at communication with professional antigen-presenting cells, including myeloid cells and B cells[7].

The response of both CD8+ cytotoxic T lymphocytes (CTLs) and antibody-producing B cells relies on CD4+ T-cell help, which is delivered during priming in dLNs and spleen[8,9]. CD4+ and CD8+ T-cell priming is the resultant of multiple T cell-DC interactions involving different cDC types. The cDC2s excel at antigen presentation in MHC-II molecules and are generally important for initial CD4+ T-cell activation[10,11], while cDC1s have superior capacities for processing and presenting exogenous cell-associated antigens in MHC-I molecules, a process called cross-presentation[12,13]. Therefore, cDC1s are important for CD8+ T-cell activation[11,14]. CD4+ and CD8+ T cells can initially be activated by separate cDC types, but in response to chemokine cues, they can engage subsequently in antigen-specific interactions with the same (r)cDC1[15,16]. In this scenario, CD4+ T cells deliver help for CTL-effector and memory differentiation[8,17] by optimizing the antigen-presenting and costimulatory capacities of the cDC1[13,18]. Interactions between CD40L on the activated CD4+ T cell and CD40 on the cDC1, as well as interferon (IFN)-I signals, are key in this help/"licensing" process[17,19–22]. CD4+ T-cell help instills via the cDC1 in CD8+ T cells optimal cytotoxic and effector-memory functions via specific transcriptional programs[23,24].

Next to cDCs, other innate cell populations can directly or indirectly impact T-cell responses during priming. For example, plasmacytoid (p)DCs provide IFN-I to cDC1 cells to optimize help for the $CD8^+$ T-cell response[25]. In addition, upon infection or inflammation with diverse pathogens and/or delivery of type I inflammatory signals, monocytes were found to infiltrate the dLN and differentiate locally into $CD11c^+MHC\text{-}II^+$ monocyte-derived (Mo)DCs[26–28]. Monocytes also infiltrate the site of infection and likewise form MoDCs locally[27–32]. Whereas monocytes exit the bone marrow in a CCR2-dependent manner[33], their recruitment to the dLN can occur both on basis of CCR2 binding to CCL2[34] or by CCR2-independent mechanisms[27,33,35–37]. The mode of recruitment from the circulation may depend on the anatomical location of the dLN[27].

In various model systems, MoDCs promoted $CD8^+$ and/or $CD4^+$ T-cell responses, quantitatively and/or qualitatively[26–29,38,39]. Several studies using adoptively transferred monocytes show that MoDC progeny of these cells perform antigen uptake and delivery to dLN[36,40,41]. However, it is debated how efficient MoDCs are at antigen-presentation and T-cell priming[37], particularly in view of the recent identification of a subset of 'inflammatory' cDC2s, which are bona fide cDCs, but are phenotypically very similar to MoDCs[42]. *In vitro* co-culture models have shown that MoDCs loaded with exogenous antigen can induce T-cell activation, but are less competent than cDCs in T-cell priming, particularly in response to cell-associated antigens[13,43]. *In vivo*, injected monocytes were observed to transport bacterial antigen to lymph nodes, but cDCs were responsible for $CD4^+$ T-cell priming[36]. Current data argue that MoDCs modulate the T-cell response subsequent to cDC-mediated *de novo* activation, particularly in terms of effector differentiation[26,39]. MoDCs can make specific cytokines including IL-12, express CD40 and various costimulatory ligands and are therefore likely candidates to help shape T-cell responses[44]. IL-12 production by MoDCs has been implicated in promoting T-cell effector differentiation[26,39]. In this study, we demonstrate that the communication between activated $CD4^+$ T cells and MoDCs is bidirectional: MoDCs respond to $CD4^+$ T-cell help via CD40- and IFNg signaling, creating a feed-forward loop for Th1 effector differentiation.

Results

The vaccination model system and myeloid cell detection

To determine the impact of $CD4^+$ T-cell help on myeloid cell populations in the priming LN, we used a vaccination model that has previously revealed the effects of $CD4^+$ T-cell help on effector and memory $CD8^+$ T-cell responses[23,24,45]. In this model, mice are vaccinated with plasmid DNA encoding the relevant antigens by "tattoo" application in depilated skin, on days 0, 3 and 6. This procedure leads to expression of the vaccine-encoded

protein in keratinocytes, its permeation to the dermis and its passive drainage, as well as active delivery by cDCs to the dLN[46]. The vaccination procedure is very potent, since the plasmid DNA delivered into the cytosol of keratinocytes acts as a DAMP and the skin damage by the tattoo needles likely also contributes to innate immune cell activation. Delivery of vaccine antigens to cDCs in the dLN occurs within 24 h post-vaccination[46]. We use two different vaccines that both encode a gene-shuffled version of the human papilloma virus (HPV)16-E7 protein including the immunodominant MHC-I restricted epitope $E7_{(48-57)}$. The Help vaccine encodes in addition linked dominant MHC-II-restricted helper epitopes including PADRE[47], while the No Help vaccine does not[48] (**Figure 1A**). Comparing the effects of these two vaccines side-by-side allowed us to directly assess the contribution of $CD4^+$ T-cell activation to the immune response. The $CD4^+$ T cells adopt a Th1 effector phenotype in this model[45]. To follow the impact of $CD4^+$ T-cell activation on the myeloid cell compartment, we designed a spectral flow cytometry panel that reliably identifies monocyte-derived cells including MoDCs, migratory and resident cDC1s and cDC2s, pDCs and neutrophils (**Figure 1B**).

Vaccine-induced $CD4^+$ T-cell activation increases MoDC frequency in the dLN

$CD4^+$ T cells specific for the PADRE antigen were detectable in the dLN from day 4 after the first vaccination onwards in the Help setting only, thus validating the experimental set up (**Figure 2A**). The frequency of MoDCs, as defined by a $CD11b^+Ly6C^+MHC\text{-}II^{int}CD11c^+$ phenotype (**Figure 1B**) increased the day after each vaccine dose (i.e., days 1, 4 and 7) and decreased over the next two days in both Help and No Help settings (**Figure 2B**). However, on day 5 and day 7, when antigen-specific $CD4^+$ T cells had strongly expanded in response to the Help vaccine, the frequency of MoDCs was significantly higher in the dLN of mice that had received Help compared to No Help vaccination (**Figure 2B**). Zooming in on day 5 post vaccination, the frequency of total $Ly6C^+CD11b^+$ monocyte-derived cells was significantly higher after Help vaccination in the dLN and not in the contralateral non-draining (nd)LN (**Figure 2C, D**). MHC-II and CD11c expression on $Ly6C^+CD11b^+$ monocyte-derived cells in the dLN was higher than in the ndLN in both Help and No Help vaccination settings (**Figure 2E**). These findings align with earlier observations that upon type 1 immune challenges by infection or adjuvants, $Ly6C^+CD11b^+$ monocytes enter the dLN from blood and locally differentiate into MoDCs that have increased expression of MHC-II and CD11c[26,27,49]. The majority of monocytic cells found in the dLN at day 5 after vaccination had a $Ly6C^+CD11b^+MHC\text{-}II^{int}CD11c^+$ phenotype and their frequency was higher in the Help setting than in the No Help setting (**Figure 2F**). Help vaccination did not alter the frequencies of migratory and resident cDC1s and cDC2s, as compared to No Help vaccination (**Supplementary Figure 1A**). In both vaccination settings, the frequency of migratory cDC2s was higher in the dLN than in the ndLN (**Supplementary**

Figure 1A). Neutrophil frequencies were comparable after Help and No Help vaccination (**Supplementary Figure 1B**), while pDC frequencies were lower after Help vaccination, in both dLN and ndLN (**Supplementary Figure 1C**).

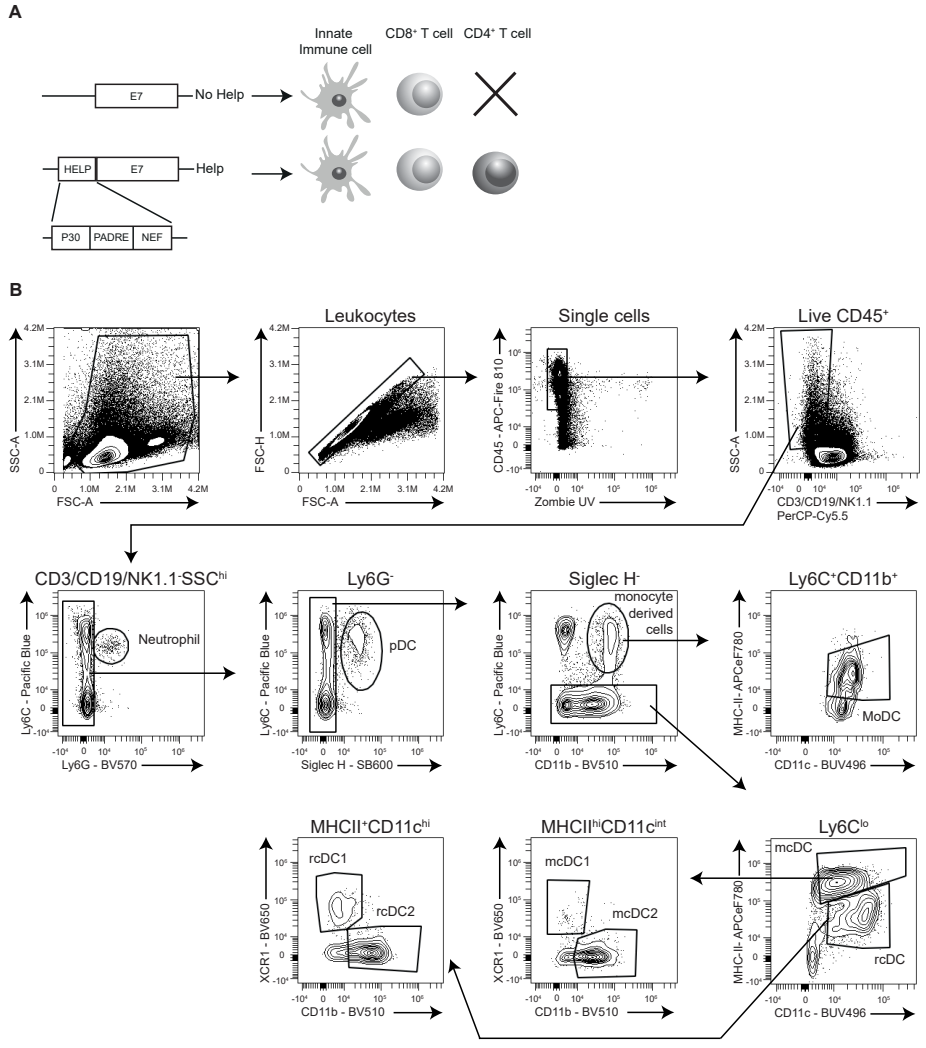

Figure 1. Vaccination model system and flow cytometric gating of myeloid cell populations.
(A) Schematic representation of Help or No Help DNA vaccine constructs and immune cell engagement. The indicated helper epitopes P30, PADRE and NEF were selected on human HLA-DP, -DR and DQ-binding. P30 and PADRE epitopes also bind to MHC-II in C57BL/6 mice[47,74]. PADRE is a synthetic epitope consisting of amino acids AKFVAAWTLKAA and is presented by H2-IA^{b}. The HPV-E7 protein is encoded by a shuffled gene to avoid cell transformation upon transfection and encodes one immunogenic H2-D^{b}-restricted epitope E7$_{49-57}$ (RAHYNIVTF) and no helper epitopes, as validated in[48]. **(B)** Representative gating strategy for detection of monocyte-derived cells and MoDCs, migratory and resident cDC1s and cDC2s, pDCs and neutrophils. Mice were vaccinated with Help or No Help at day 0 and day 3. At day 5, single cell suspensions of dLN and ndLN were analyzed. Data presented are from a representative dLN sample vaccinated with No Help.

To correctly define MoDCs, we used a set of lineage-specific markers that discern MoDCs from rcDC1s and rcDC2s and from the recently described inflammatory cDC2s[42]. In both Help and No Help settings, levels of MHC-II and CD11c on MoDCs were comparable to those on rcDC1s, while levels of CCR2 and CD64, markers of monocytic cells and inflammatory cDC2s[1,2,42] were higher on MoDCs than on rcDC1s and rcDC2s (**Figure 2G**). Levels of these markers on MoDCs did not differ between Help and No Help settings (**Supplementary Figure 1D**). Low CD26 levels discriminated MoDCs as monocyte-derived cells from cDC1s and (inflammatory) cDC2s (**Figure 2G**), as defined previously[42,50]. Furthermore, MoDCs lacked the cDC-restricted transcription factor Zbtb46[51] as well as IRF8 and IRF4, which define cDC1 and cDC2 lineages, respectively[50] (**Figure 2G**). Altogether, our data argue that the vaccination procedure induces a MoDC response in the dLN, which is significantly enhanced by CD4+ T-cell help. The MoDCs likely differentiate in the dLN from monocytes that are recruited from the blood, as described previously[26,27].

Monocyte-derived cells optimize CD4+ T-helper 1 and CD8+ effector differentiation

To investigate the possible impact of monocyte-derived cells on T-cell effector differentiation in the dLN after Help vaccination, we treated mice with an antibody directed at CCR2 (**Figure 3A**). The low dose of anti-CCR2 antibody used depletes monocytes from the circulation[52,53] and effectively depleted MoDCs (**Figure 3B-C).** CCR2 was expressed at high level on monocytes and at low levels on migratory and resident cDC1s and cDC2s (**Supplementary Figure 2C**). Treatment with anti-CCR2 antibody did not affect cDC frequencies within the dLN (**Supplementary Figure 2D**). Among monocyte-derived cells, we did not detect macrophages as defined by F4/80 staining in the dLN after vaccination (results not shown). CCR2 was not expressed on PADRE-specific CD4+ T cells (**Supplementary Figure 2E**) and antibody treatment did not affect the frequency of these cells after vaccination (**Figure 3D and Supplementary Figure 2F**). We can conclude from these data that MoDC depletion did not affect clonal expansion of PADRE-specific CD4+ T cells. However, inhibition of the MoDC response did impede differentiation of responder CD4+ T cells into Th1 cells. This was apparent from a reduced frequency of PADRE-specific CD4+ T cells with a SLAM+T-bet+ Th1 phenotype (**Figure 3E, F**) and a reduced frequency of IFNγ-producing CD4+ T cells after restimulation *in vitro* with either PADRE peptide, or with agonistic antibodies to CD3 and CD28 (**Figure 3G, H**). Inhibition of the MoDC response also led to a reduction in the frequency of HPV E7-specific CD8+ T cells in blood and spleen, but not in dLNs (**Figure 3I, Supplementary Figure 2G**). HPV E7-specific CD8+ T cells in blood and spleen were enriched for a KLRG1+CX3CR1+ effector phenotype as compared to those in the dLN (**Figure 3J, Supplementary Figure 2H**), which is consistent with primed CD8+

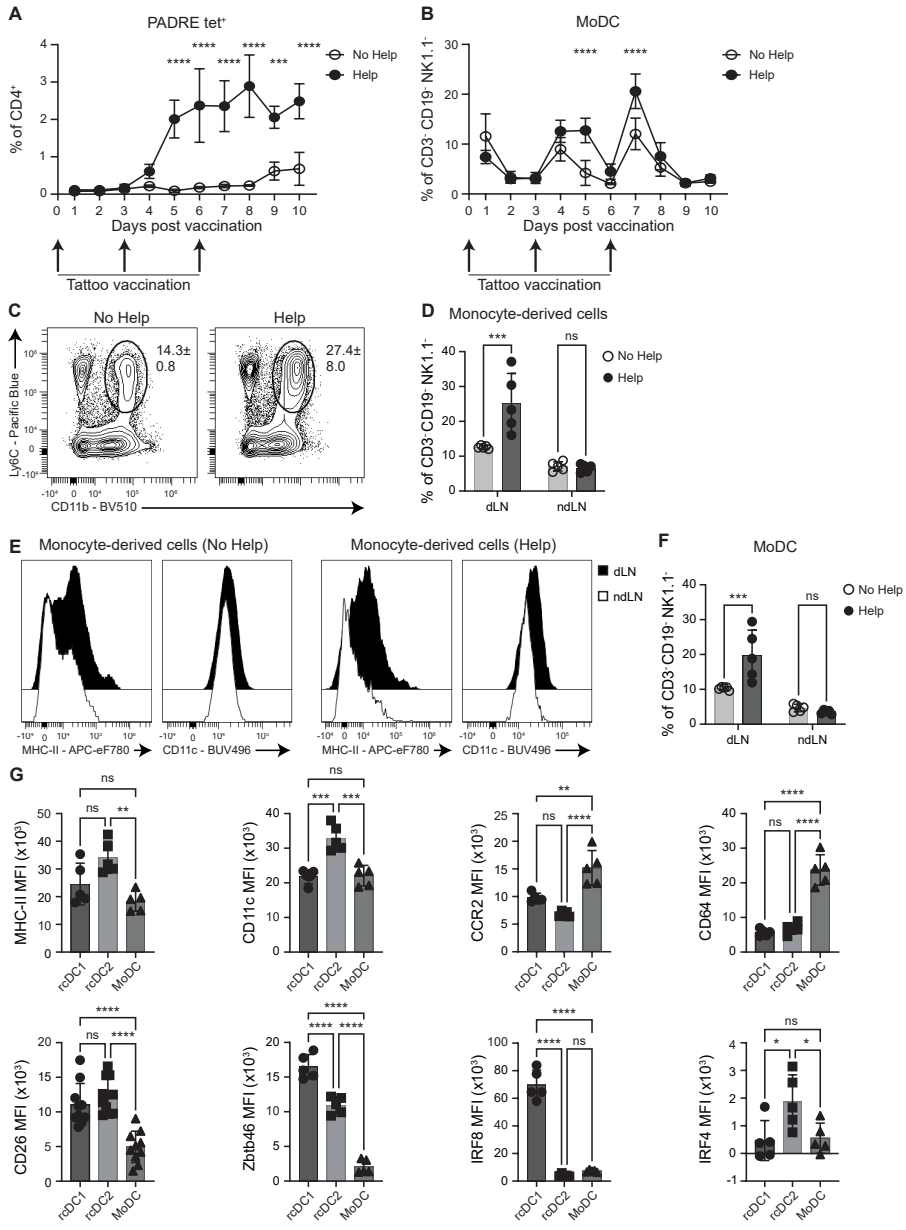

Figure 2. CD4⁺ T-cell priming stimulates a MoDC response after vaccination.
(A, B) Frequency of H2-IA^b/PADRE tetramer (tet)$^+$ CD4$^+$ T cells (A) and Ly6C$^+$CD11b$^+$MHC-II^{int}CD11c$^+$ MoDCs (B) in the dLN of mice as detected by flow cytometry at the indicated days after Help or No Help vaccination on day 0, 3 and 6 (arrows). N = 3 mice per group (mean ± SD), representative of two independent experiments. **(C-G)** Mice received Help or No Help vaccine and dLN were analyzed by flow cytometry at day 5 post vaccination. **(C, D)** Contour plots (C) and quantification (D) of Ly6C$^+$CD11b$^+$Ly6G$^-$ monocyte-derived cells within CD3$^-$CD19$^-$NK1.1$^-$ cells. **(E)** Representative histograms showing expression levels of MHC-II and CD11c on monocyte-derived cells from dLN or ndLN of mice vaccinated under Help or No Help conditions.

(F) Quantification of Ly6C+CD11b+MHC-IIintCD11c+ MoDCs in dLN and ndLN. **(G)** MFI of indicated markers on rcDC1s, rcDC2s and MoDCs from dLN of mice that received Help vaccine. Statistics: (A) N = 3 mice (No Help) or N = 8 mice (Help) (mean ± SD); representative of one experiment (No Help) or pooled from two independently performed experiments, (B) N = 3 mice per group (mean ± SD);, representative of two independently performed experiments; (C-G) N = 5 mice per group (mean ± SD), representative of at least two independently performed experiments; (A, B, D, F) Two-way ANOVA with Sidak post hoc test to correct for multiple testing; (G) One-way ANOVA with Tukey post hoc test to correct for multiple testing.

T cells leaving the dLN to the blood after completing their effector differentiation. The frequency of KLRG1+CX3CR1+ CD8+ T cells in blood and spleen was significantly reduced upon abrogation of the MoDC response. Altogether, these data argue that in our vaccination model, MoDCs in the dLN do not affect initial activation of vaccine-specific CD4+ and CD8+ T cells, which is likely induced by cDCs. However, MoDCs in the dLN promote local T-cell effector differentiation. Thus, by boosting the MoDC response, activated CD4+ T cells enhance their own proinflammatory Th1 type effector differentiation and the formation of effector CD8+ T cells.

CD4+ T-cell activation alters costimulatory molecule expression on monocyte-derived cells

It has been described that MoDCs can express a diversity of costimulatory molecules[44]. CD40, CD28 ligands CD80 and CD86, as well as co-inhibitory ligand PD-L1 were upregulated on monocyte-derived cells in the dLN at day 5 days post vaccination (**Figure 4A**). These molecules are known to be upregulated by CD4+ T-cell help on cDCs[8,17–19] and we therefore compared their expression on monocyte-derived cells after Help or No Help vaccination. On day 5 post-vaccination, CD4+ T-cell activation had led to higher expression of CD80 (**Figure 4B**), while CD86 expression was modestly lowered (**Figure 4C**). CD4+ T-cell activation increased the frequency of both CD40+ and PD-L1+ monocyte-derived cells, as well as the expression level of these molecules per cell (**Figure 4D, E**). It also increased the frequency of CD80+PD-L1+ monocyte-derived cells (**Figure 4F**), which suggests a better costimulatory status, as will be explained in the Discussion. These results indicate that vaccine-induced MoDCs upregulate costimulatory molecules and that activation of CD4+ T cells not only augments the number of MoDCs in the dLN, but furthermore increases their potential to costimulate T-cells and to respond to CD40L input.

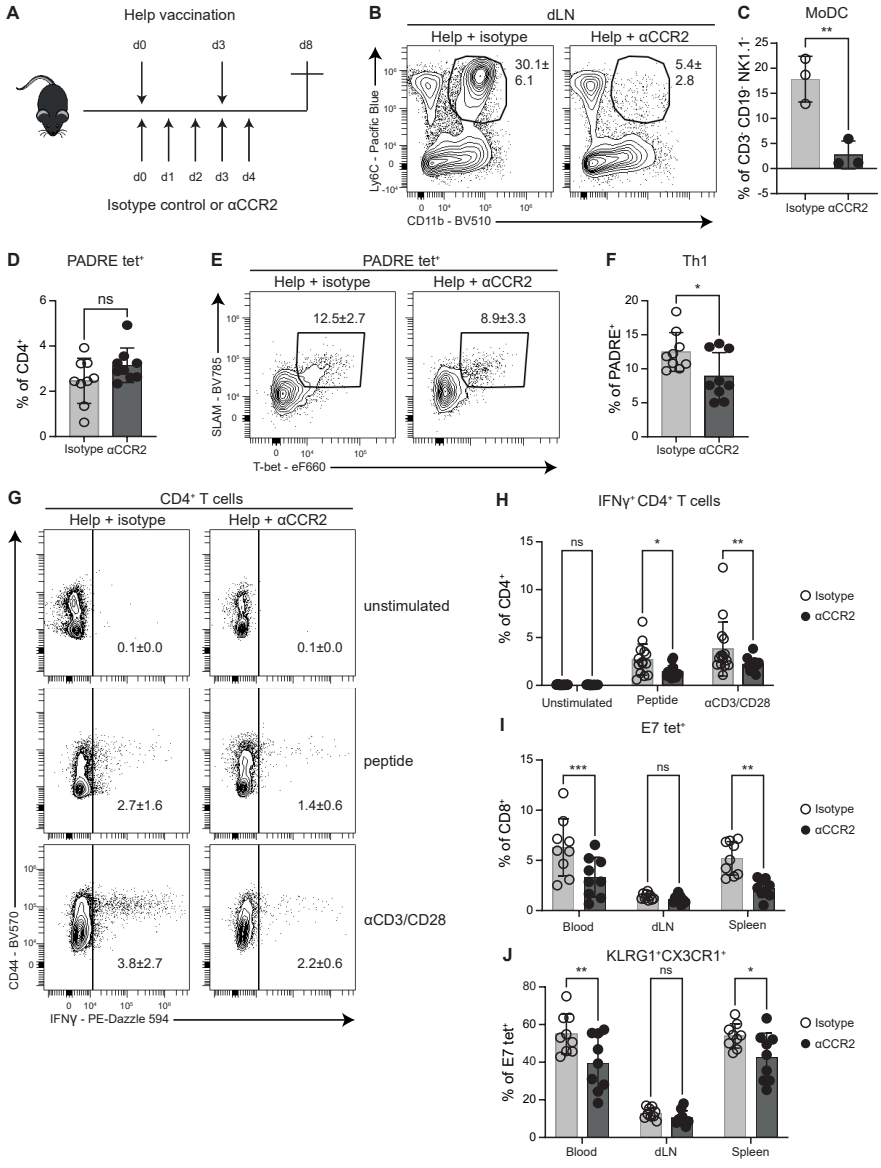

Figure 3. Monocyte-derived cells promote CD4⁺ and CD8⁺ T-cell effector differentiation.
(A) Experimental design including vaccination and treatment with antibody to CCR2. **(B)** Contour plots representing Ly6C⁺CD11b⁺Ly6G⁻ monocyte-derived cells among CD3⁻CD19⁻NK1.1⁻ cells at day 4. **(C)** Graph depicting the frequency of Ly6C⁺CD11b⁺MHC-II^{int}CD11c⁺ MoDCs in the dLN at day 4. **(D)** Quantification of H2-IA^{b}/PADRE tet⁺ CD4⁺ T cells at day 8. **(E, F)** Representative contour plots (E) and quantification (F) of Th1 (SLAM⁺T-bet⁺) cells within H2-IA^{b}/PADRE tet⁺ CD4⁺ T cells at day 8. **(G, H)** Representative contour plots (G) and quantification (H) of IFNγ production as determined by intracellular staining of cells isolated from dLNs at day 8 and over-night stimulated in vitro as indicated. **(I, J)** Frequency of H2-D^{b}/E7 tet⁺ CD8⁺ T cells (H) and KLRG1⁺CX3CR1⁺ cells within H2-D^{b}/E7 tet⁺ CD8⁺ T cells (I) in indicated organs. Statistics: (B, C) N = 3 mice per group representative of one experiment. (D-F) N = 9 mice per group (mean ± SD) representative of two independently performed experiments; (G-H) N = 15 mice per group (mean ± SD) representative of one experiment; (I-J) N = 9

mice per group (mean ± SD) representative of three independently performed experiments; (C, D, F) Unpaired student t-test; (G-J) Two-way ANOVA with Sidak post hoc test to correct for multiple testing.

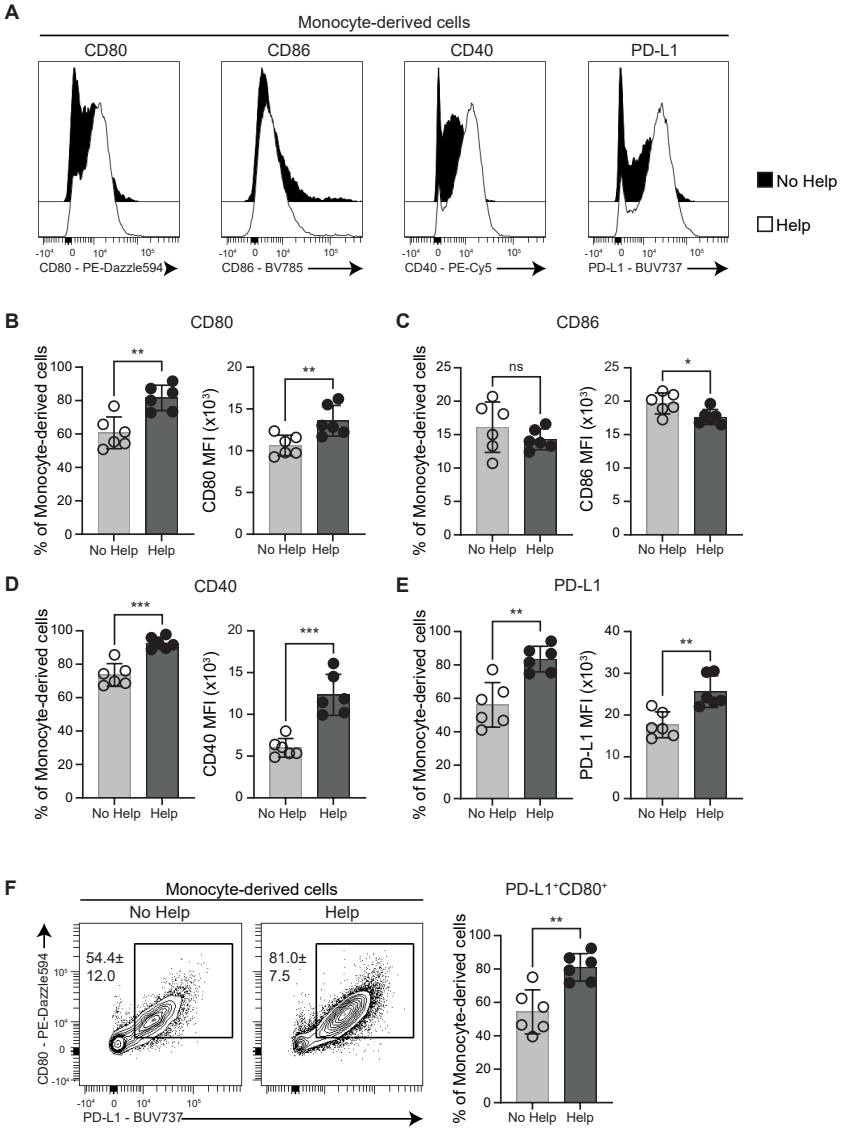

Figure 4. CD4+ T-cell priming promotes the costimulatory status of monocyte-derived cells.
(A) Histograms indicating expression levels of CD80, CD86, CD40 and PD-L1 on total monocyte-derived cells day 5 post vaccination. **(B-E)** Bar graphs depicting expression of CD80 (B), CD86 (C), CD40 (D) and PD-L1 (E) on monocyte-derived cells in the dLN. Left: frequency of positive cells; right: MFI of the positive cell population. **(F)** Contour plot and quantification displaying CD80 and PD-L1 co-expression by monocyte-derived cells. Analysis was done at day 5 in dLN. Statistics: N = 6 mice per group (mean ± SD), representative of three independently performed experiments; Unpaired student t-test. Histograms are a concatenation from dLNs of 6 mice.

Activated CD4$^+$ T cells enhance the MoDC response via CD40-CD40L interactions and IFNγ

CD4$^+$ T cells quickly upregulate CD40L upon antigen recognition and via CD40 signaling license cDC1s for optimal induction of CTL effector and memory responses[17,19–22]. Given that MoDCs upregulated CD40 in response to Help vaccination, we hypothesized that CD4$^+$ T cells may boost the innate MoDC response via CD40L/CD40 interactions. Furthermore, because it has been shown that NK cells can boost the MoDC response via IFNγ[32,49,54], we also hypothesized a role for IFNγ production by CD4$^+$ T cells herein. To assess whether CD40/CD40L interactions or IFNγ signaling were instrumental in the Help-mediated MoDC response, we treated mice during Help vaccination with blocking antibodies against CD40L or IFNγ or isotype controls and included for reference the No Help vaccination setting. Five days after vaccination, the frequency of CD11b$^+$Ly6C$^+$ monocytes that had entered the dLN was significantly reduced in mice that were treated anti-CD40L antibody (**Figure 5A, B**). This was associated with a significant reduction of the MoDC response that fell back to the levels of No Help-vaccinated mice (**Figure 5C**). In contrast to CD40L blockade, IFNγ blockade did not affect the influx of monocyte-derived cells to the dLN (**Figure 5A, B**), but specifically hampered MoDC differentiation to a similar extent as anti-CD40L blockade (**Figure 5C**).

CD40L or IFNγ blockade also reduced the CD40, CD80 and PD-L1 expression on monocyte-derived cells in the Help setting to the levels observed in the No Help setting, thus neutralizing the effect of activated CD4$^+$ T cells on phenotype. Antibody treatment did not affect CD86 levels (**Figure 5D, E**). NK cell depletion with NK1.1 antibody successfully depleted NK cells (**Supplementary Figure 3A, B**), but did not significantly affect the MoDC response (**Figure 5F**), suggesting a primary role for CD4$^+$ T cell-mediated IFNγ production in boosting the MoDC response in the dLN. Altogether, we show that upon DNA vaccination into the skin, vaccine-activated CD4$^+$ T cells promote a MoDC response in the vaccine-dLNs. Activated CD4$^+$ T cells promote generation of MoDCs in the dLN and improve the costimulatory status of monocyte-derived cells. The monocyte-derived cells are not required for initial activation of CD4$^+$ and CD8$^+$ T cells, which is likely mediated cDCs. MoDCs however locally enhance Th1 type CD4$^+$ and CD8$^+$ effector differentiation of vaccine-specific T cells. Importantly, activated CD4$^+$ T cells act in a feed-forward loop and crosstalk with MoDCs through CD40/CD40L interaction and IFNγ-mediated signaling (**Figure 5G**).

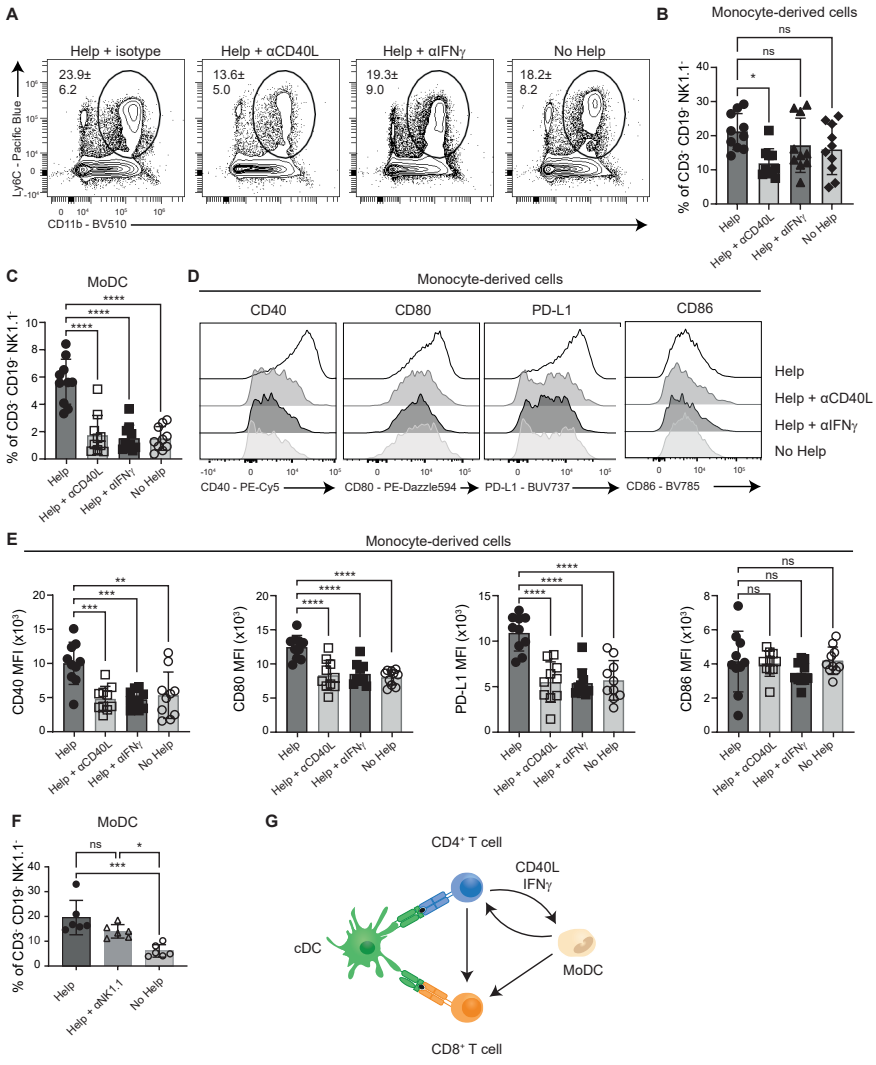

Figure 5. Primed CD4⁺ T cells promote the MoDC response via CD40L and IFNγ.
(A-E) Mice received Help vaccination and were treated with blocking antibodies to CD40L, IFNγ, or isotype control on day 0 and 3, or with depleting antibody to NK1.1 on day -1, 0 and 3, and analyzed at day 5. Mice receiving No Help vaccination served as a reference. **(A)** Contour plots representing Ly6C⁺CD11b⁺Ly6G⁻ monocyte-derived cells. **(B, C)** Graph depicting the frequency of Ly6C⁺CD11b⁺Ly6G⁻ monocyte derived cells (B) or Ly6C⁺CD11b⁺MHC-II^{int}CD11c⁺ MoDCs (C) in the dLN 5 days post vaccination. **(D, E)** Representative histograms (D) and quantification (E) of CD40, CD80, PD-L1 and CD86 expression levels on monocyte-derived cells. **(F)** Frequency of Ly6C⁺CD11b⁺MHC-II^{int}CD11c⁺ MoDCs in mice treated with anti-NK1.1. **(G)** Schematic representation of the findings in this study. Statistics: (B, C, E) N = 10 mice per group (mean ± SD); One-way ANOVA with Tukey post hoc test to correct for multiple testing; (E) N = 6 mice per group (mean ± SD); Two-way ANOVA with Sidak post hoc test to correct for multiple testing.

Discussion

Monocytes and DCs stem from the common myeloid progenitor (CMP) that gives rise to monocytes via specific progenitors and to pDCs, cDC1s and cDC2s via the common DC progenitor (CDP). The cDC2 lineage is now discerned into cDC2A and cDC2B subsets, of which the latter expresses a number of genes that are also associated with monocytes[55] However, all cDCs can be discerned from monocytic cells by expression of the Zbtb46 transcription factor. The recently identified ''inflammatory'' cDC2 population also closely resembles monocytes, sharing e.g. CD64 and Ly6C, but unlike monocytes expresses CD26 and lacks CCR2[42]. Given the sharing of commonly used markers, properties ascribed to *ex vivo* MoDCs may potentially be attributed to inflammatory cDC2s[37], unless MoDCs were traced from monocytes by genetic or fluorescent markers. In our study, we included in our marker panel CCR2, Zbtb46 and CD26, which confirmed the identity of the observed $CD11b^{+}Ly6C^{+}MHC\text{-}II^{int}CD11c^{+}$ cells as MoDCs.

In our model[45] both Help and No Help vaccination induced a MoDC response in the dLN. This agrees with the observation that various type I TLR agonists as innate signal sufficed to induce a MoDC response in the dLN[26]. However, $CD4^{+}$ T-cell activation by the Help vaccine significantly increased the MoDC response. In a model of i.p. infection of mice with *T. gondii*, generation of MoDCs from monocytes in the peritoneum depended on IFNγ signaling, and pinpointed NK cells as the IFNγ source[32] Similarly, inoculation with heat-killed *M. smegmatis* induced an NK cell-derived IFNγ dependent MoDC response that was critical for $CD4^{+}$ T-cell differentiation into Th1 cells[49,54]**.** In our Help vaccination setting, the MoDC response in the dLN was also IFNγ-dependent, but did not rely on NK cells, as evaluated by the same antibody-based depletion approach. This result suggests that in this case, IFNγ produced by activated $CD4^{+}$ T cells boosted the MoDC response. These findings identify a Th1-cell based feed-forward mechanism for MoDC generation via IFNγ signaling.

We found that primed $CD4^{+}$ T cells also stimulated the MoDC response via CD40. A role for CD40 signaling agrees with findings that combined CD40 and IFN-I signaling drove differentiation of monocytes into MoDCs *in vitro*[56] and CD40 agonism *in vivo* promoted a MoDC response in a mouse tumor model[57]. Collaboration between CD40L and IFN-I signaling in inducing cDC maturation has recently been shown by transcriptome analysis, where the distinct signal transduction pathways activated by the respective receptors integrated at the level of transcription factor function and resulting gene expression[58]. Likely, CD40L and IFNg collaborate in a similar fashion to promote MoDC differentiation from monocytes via their respective receptors. Since CD40L/CD40 signaling takes place during cell-cell contact[59], primed $CD4^{+}$ T cells in the dLN likely promoted MoDC differentiation from monocytes locally. The MoDCs generated in

our vaccination model upregulated CD40 as a result of CD4+ T-cell priming, again suggesting a feed-forward mechanism for MoDC generation via CD40L/CD40 signaling. CD40 signaling into monocytes can promote their activation status and functionality in terms of secretion of hallmark cytokines such as IL-12[60]. Two studies have proven by genetic deficiency that IL-12 produced by monocyte-derived cells can promote CD4+ and CD8+ effector T cell differentiation[26,39].

CD40L is rapidly and transiently expressed on CD4+ T cells upon their T-cell receptor (TCR)-mediated activation[59], which suggests a direct, possibly antigen-specific interaction between CD4+ T cells and activated monocytes/MoDCs in the dLN. Delivery of antigen from the site of infection to the dLN by activated monocytes/MoDCs has been suggested by several studies. These studies have been summarized recently and discussed in view of the identification of inflammatory cDC2s that may have been responsible for such transport[37]. In a case where adoptively transferred monocytes were proven to deliver bacterial antigen from the site of infection to the dLN, T-cell priming nevertheless relied on cDCs[36]. Recent work using CD62L blocking antibodies and surgical resection of the injection site argue for a mechanism wherein monocytes are recruited from the blood into the dLNs via high endothelial venules, locally differentiate into MoDCs[26] and acquire antigen from migratory cDCs that have sampled the site of antigen challenge[29]. Antigen transfer between different cDC types in dLNs has been documented and shown to be important for T-cell responses[61–63], in particular in the context of the two-step priming model, wherein CD4+ T-cell help is delivered in a second step of priming on cDC1, after initial CD4+ and CD8+ T-cell activation on different cDC types[8]. To this date, it is unresolved whether MoDCs present antigen to T-cells *in vivo* during the process of T-cell priming[36,40,43]. Experiments with MoDC-specific genetic deletion of MHC-II will have to resolve this issue.

In our vaccination model, MoDCs generated in the dLN boosted Th1 differentiation of the primed CD4+ T cells and effector differentiation of primed CD8+ T cells. Theoretically, macrophage offspring from CCR2+ monocytes fluxing into the dLN might have played a role in T-cell response modulation, but we did not detect any such cells in the dLN after vaccination according to F4/80 staining. Additionally, embryonically derived, tissue-resident macrophages are CCR2 independent[64,65]. Therefore, MoDCs are the most likely cell type involved. In our model, cDCs bring vaccine antigen derived from dead keratinocytes to the dLN[46], which needs to be cross-presented to CD8+ T cells. cDC1s are likely responsible for CD8+ T-cell priming, since MoDCs cannot efficiently cross-present cell-associated antigen, either in presence or absence of CD4+ T-cell help[13]. However, monocyte-derived cells can obtain MHC-I-peptide complexes via cross-dressing and stimulate CD8+ T cells as recently shown in tumor contexts[66]. This

mechanism agrees with multiple observations that MoDCs boost $CD4^+$ and $CD8^+$ T-cell responses in the dLN, but are likely not instrumental in their induction, as we also demonstrate[26,27,39,49,67]. Indeed *in vitro*, cytokine production by $CD4^+$ T cells is enhanced when T cells are activated by cDCs in presence of MoDCs[43]. The *in vivo* scenario for cooperation between cDC and MoDC in T-cell priming in response to skin challenge was recently shown to involve directed migration of rcDC2, rcDC1 and locally differentiated MoDCs to the deep T-cell zone of the dLN. Whereas rcDCs promoted initial activation and clonal expansion of $CD4^+$ and $CD8^+$ T cells, MoDCs supported effector differentiation via IL-12 production[26]. Migratory cDCs were redundant in this study that used soluble ovalbumin, but are expected to play a major role in case of cell-associated antigen.

We found that the MoDCs formed in the dLN after Help vaccination had upregulated CD80 and PD-L1. Importantly, PD-L1 does not indicate a tolerogenic state of DCs, since it can form a heterodimer *in cis* with CD80[68]. Once part of this heterodimer, CD80 can no longer be downregulated by CTLA-4 and PD-L1 can no longer bind to PD-1[69]. The CD80:PD-L1 heterodimer retains the ability to signal via CD28 and thereby forms an immunostimulatory signaling molecule[70]. Future studies should examine the costimulatory nature of MoDCs after $CD4^+$ T-cell help aspect more extensively, particularly in terms of expression of TNF family ligands and cytokines that are important for effector differentiation of $CD4^+$ and $CD8^+$ T cells, as documented for cDCs[71]. Next to IL-12, multiple specific cytokines and chemokines that are important in T-cell differentiation can be made by monocyte-derived cells[26,39,49,72,73], and may complement cDC function, or even substitute for it in specific cases[66]. Additionally, licensing of cDC1s by $CD4^+$ T-cell help involves many additional mechanisms that promote T-cell effector and memory fate[8,13,17,18], and it will be of interest to determine which of these can be boosted by MoDCs. In conclusion, the collective data argue that the MoDC response that takes place under type I inflammatory conditions in dLNs can be boosted not only by innate mechanisms, but also by an adaptive mechanism involving $CD4^+$ T cells, IFNγ and CD40L signaling. The MoDC response is not primarily responsible for T-cell priming but supports T-cell effector differentiation in a feed-forward loop induced by Th1 type $CD4^+$ T-cell activation.

Methods

Mouse maintenance and antibody treatment

Eight-week-old female C57BL/6JRj mice were purchased from Janvier laboratories (Le Genest Saint Isle, France). Mice were housed in individually ventilated cages (IVC) under specific pathogen-free (SPF) conditions and with *ad libitum* access to food and water. Ambient temperature was ~19-21 °C and humidity 30-70%. Lighting was provided on a 12 h light/dark cycle. All mouse experiments were performed in accordance with institutional and national guidelines and were approved by the Animal Welfare Body at Leiden University Medical Center. Antibodies were injected intraperitoneally (i.p.). Mice received injections with 20 µg depleting anti-CCR2 (clone MC-21[52,53] or rat IgG2b isotype control (clone LFT-2, BioXcell) in 100 µl PBS daily from day 0 to 4. Mice received injections with 150 µg blocking anti-CD40L (clone MR-1, BioXcell) or 200 µg anti-IFNγ (clone XMG1.2, BioXcell) or 200 µg rat IgG1 isotype control (clone HRPN, BioXcell) in 100 µl PBS on day 0 and day 3 post vaccination. Mice received injections with 100 µg depleting anti-NK1.1 (clone PK136, produced in house) in 100 µl PBS starting at 1 day prior to vaccination and on day 0 and day 3 after the first vaccination.

DNA tattoo vaccination and tissue processing

HELP-E7SH and E7SH pVAX1 plasmid vaccines were generated as described[48]. The amino acid sequences they encode and the validation of the procedure are provided in[45]. For intraepidermal DNA tattoo vaccination, mice were anesthetized using isoflurane (Induction phase; 4% isoflurane, airflow 0.8 L/min. Maintenance phase; 2% isoflurane, airflow 0.4 L/min) maintenance and the right hind leg of mice was depilated using Veet containing limonene (Reckitt Benckiser). Subsequently, 15 µl of 2 mg/ml plasmid DNA in H_2O was tattooed into the skin with a Permanent Make Up tattoo machine (Cheyenne, MT Derm GmbH) using a sterile disposable 9-needle bar with a needle depth of 1 mm. Tattooing was performed for 45 s, oscillating at a frequency of 100 Hz. Mice were vaccinated at day 0, 3 and 6, unless otherwise indicated, and alternating between the internal or external upper part of the right hind leg. On the day of read out, mice were euthanized by means of CO_2 inhalation and organs collected. Blood was collected by tail vein puncture and collected in heparin coated Microvette CB300 LH tubes (Sarstedt). Erythrocytes were lysed by incubation in red blood cell lysis buffer (Santa Cruz) for 2 × 5 min at room temperature. Inguinal dLN were punched repeatedly with a 25 G needle (BD) and incubated in 500 µl DMEM (Gibco) with 100 µg/ml Liberase TL (Roche) for 30 min at 37 °C while shaking. Enzymatic digestion was quenched by adding IMDM (Gibco) with 10% FBS and single cell suspensions were prepared by mechanic disruption of the dLN through a 70 µM Falcon® cell strainer (Corning).

Flow cytometry

For cell surface staining, antibodies were diluted in FACS buffer (PBS + 2% FBS), and staining was performed in 96 well U bottom plates (Greiner). Dead cell exclusion was done using 1:500 Zombie UV fixable viability dye (Biolegend) or 1:1000 LIVE/DEAD NIR fixable viability dye (Invitrogen). For analysis of myeloid populations, single cell suspensions were first incubated with 1:50 anti-mouse Fc Block™ (anti-CD16/32, clone 2.4G2, 1:50 BD) for 5 min on ice, while for antigen-specific $CD4^+$ T cell analysis, single cell suspensions were first incubated for 1 h at room temperature with PE-conjugated PADRE tetramer (AKFVAAWTLKAA in H-2I-A^b, 1:200, NIH tetramer facility) in FACS buffer. For cytokine restimulation, 96 flat bottom plates (Corning) were coated with 2 ug/ml agonistic antibodies to both CD3 (clone 145-2C11, Biolegend) and CD28 (clone 37.51, Biolegend) in PBS overnight at 4 degrees or left untouched. The next day, 0.5×10^6 dLN derived single cells were incubated on anti-CD3 and anti-CD28 coated plates or with 1 µM PADRE peptide (AKFVAAWTLKAA) on uncoated plates or left unstimulated in IMDM + 10% FCS + 50 units/ml Penicillin-Streptomycin (Gibco) for 16 h. Subsequently, samples were incubated with 1:1000 GolgiPlug™ with Brefeldin A (BD) for 2 h. Subsequently, single cell suspensions were incubated for 30 min on ice with the following fluorochrome-conjugated monoclonal antibodies in FACS buffer: CCR2 BUV661 (clone 475301; 1:200), CD11c BUV496 (clone HL3; 1:100), CD115 BUV615 (clone ASF98; 1:200), CD26 (clone H194-112; 1:100), CD4 BUV805 (clone GK1.5; 1:200), CD8α BV750 (clone 53-6.7; 1:200), CD8a V500 (clone 53-6.7; 1:100), KLRG1 BUV563 (clone 2F1; 1:100), PD-L1 (clone MIH5; 1:200), SIRPα BUV395 (clone P84; 1:100), all from BD, CD11b BV510 (clone M1/70; 1:200), CD19 PerCP-Cy5.5 (clone 6D5; 1:400), CD3 PerCP-Cy5.5 (clone 17A2; 1:100), CD40 PE-Cy5 (clone 3/23; 1:100), CD44 BV570 (clone IM7; 1:100), CD44 BV785 (clone IM7; 1:100), CD45 APC-Fire 810 (clone 30-F11; 1:200), CD64 AF647 (clone X54-5/7.1; 1:100), CD80 PE-Dazzle 594 (clone 16-10A1; 1:100), CD86 BV785 (clone GL-1; 1:200), CX3CR1 BV421 (clone SA011F11; 1:800), CX3CR1 PerCP-Cy5.5 (clone SA011F11; 1:200), Ly6C Pacific Blue (clone HK1.4; 1:800), Ly6G BV570 (clone 1A8; 1:100), NK1.1 PerCP-Cy5.5 (clone PK136; 1:100), NKp46 PE-Dazzle 594 (clone 29A1.4; 1:50), SLAM BV785 (clone TC15-12F12.2; 1:100), XCR1 BV650 (clone ZET; 1:100), all from Biolegend, KLRG1 PE-eFluor 610 (clone 2F1; 1:200), MHC-II APC-eFluor 780 (clone M5/114.15.2; 1:2000), Siglec H Super bright 600 (clone eBio440c; 1:100) all from Invitrogen, and APC-conjugated E7 tetramer ($E7_{49\text{-}57}$, RAHYNIVTF in H2-D^b, 1:100 produced in house). Intracellular staining was performed using the Foxp3/Transcription factor staining kit (eBioscience) according to the manufacturers provided protocol. Cells were fixed and permeabilized for 30 min on ice and subsequently intracellularly stained for 30 min on ice with the following antibodies IFNγ PE-Dazzle 594 (clone XMG1.2, Biolegend, 1;400) IRF4 PerCP-eFluor 710 (clone 3E4, eBioscience, 1:1200), IRF8 APC (clone V3GYWCH, Invitrogen, 1:100), T-bet eFluor 660 (clone eBio4B10, eBioscience,

1:200) and Zbtb46 PE (clone U4-1374, BD, 1:100). Data were acquired using a Cytek Aurora Spectral 3-laser equipped with, 405 nm, 488 nm, and 640 nm lasers (Cytek Biosciences) or a Cytek Aurora Spectral 5-laser Flow Cytometer equipped with 355 nm, 405 nm, 488 nm, 561 nm and 640 nm lasers (Cytek Biosciences), and analyzed with OMIQ (Dotmatics, version 2024.07) or FlowJo software (TreeStar, version 10.8.1).

Statistics

In graphs, mean±SD are depicted. For protein expression depiction, median fluorescent intensity (MFI) is used. Statistical analysis was performed with GraphPad Prism 9.3.1 (Dotmatics) using two-tailed unpaired Student *t*-test when comparing two groups, One-Way ANOVA with Tukey post hoc test to correct for multiple testing when comparing multiple groups at one timepoint or Two-Way ANOVA with Sidak post hoc test to correct for multiple testing when comparing groups at different timepoints, or multiple organs between groups. P values < 0.05 were considered statistically significant Statistics were denoted as follows; *; $P \leq 0.05$, **; $P \leq 0.01$, ***; $P \leq 0.001$ and ****; $P \leq 0.0001$. If no significance is indicated, this is considered not significant, $P > 0.05$.

Data Availability

Flow cytometry data that further support the findings this study are available upon request.

Author contributions

Douwe M. T. Bosma: Writing – review & editing, Writing – original draft, Visualization, Validation, Methodology, Investigation, Formal analysis, Conceptualization. **Julia Busselaar:** Writing – review & editing, Methodology, Investigation. **Mo D. Staal:** Writing – review & editing, Methodology, Investigation. **Elselien Frijlink:** Writing – review & editing, Methodology, Investigation. **Matthias Mack:** Methodology. **Fiamma Salerno:** Writing – review & editing, Writing – original draft, Visualization, Methodology, Investigation, Formal analysis, Conceptualization. **Jannie Borst:** Writing – review & editing, Writing – original draft, Validation, Supervision, Project administration, Investigation, Funding acquisition, Conceptualization.

Acknowledgments

We thank the Flow Cytometry and Experimental Animal facilities of the LUMC for outstanding technical assistance and Dr. Joke den Haan (Amsterdam UMC) for advice. This research was supported by Oncode and grants 10894 and 11079 from the Dutch Cancer Society to J. Bo and a NWO-VENI grant (ZonMw project 09150162010046) to F.S.

References

1. Backer, R. A., Probst, H. C. & Clausen, B. E. Classical DC2 subsets and monocyte-derived DC: Delineating the developmental and functional relationship. *Eur J Immunol* 53, (2023).
2. Cabeza-Cabrerizo, M., Cardoso, A., Minutti, C. M., Pereira Da Costa, M. & Reis E Sousa, C. Dendritic Cells Revisited. *Annu Rev Immunol* 39, 131–166 (2021).
3. Bosteels, V. & Janssens, S. Striking a balance: new perspectives on homeostatic dendritic cell maturation. *Nat Rev Immunol* https://doi.org/10.1038/S41577-024-01079-5 (2024) doi:10.1038/S41577-024-01079-5.
4. Gerner, M. Y., Casey, K. A., Kastenmuller, W. & Germain, R. N. Dendritic cell and antigen dispersal landscapes regulate T cell immunity. *J Exp Med* 214, 3105–3122 (2017).
5. Gerner, M. Y., Kastenmuller, W., Ifrim, I., Kabat, J. & Germain, R. N. Histo-cytometry: a method for highly multiplex quantitative tissue imaging analysis applied to dendritic cell subset microanatomy in lymph nodes. *Immunity* 37, 364–376 (2012).
6. Krishnaswamy, J. K., Alsén, S., Yrlid, U., Eisenbarth, S. C. & Williams, A. Determination of T Follicular Helper Cell Fate by Dendritic Cells. *Front Immunol* 9, (2018).
7. Hilligan, K. L. & Ronchese, F. Antigen presentation by dendritic cells and their instruction of CD4+ T helper cell responses. *Cell Mol Immunol* 17, 587–599 (2020).
8. Borst, J., Ahrends, T., Bąbała, N., Melief, C. J. M. & Kastenmüller, W. CD4+ T cell help in cancer immunology and immunotherapy. *Nat Rev Immunol* 18, 635–647 (2018).
9. Duckworth, B. C. & Groom, J. R. Conversations that count: Cellular interactions that drive T cell fate. *Immunol Rev* 300, 203–219 (2021).
10. Tatsumi, N., Codrington, A. L., El-Fenej, J., Phondge, V. & Kumamoto, Y. Effective CD4 T cell priming requires repertoire scanning by CD301b+ migratory cDC2 cells upon lymph node entry. *Sci Immunol* 6, (2021).
11. Dudziak, D. *et al.* Differential antigen processing by dendritic cell subsets in vivo. *Science* 315, 107–111 (2007).
12. Den Haan, J. M. M., Lehar, S. M. & Bevan, M. J. CD8(+) but not CD8(-) dendritic cells cross-prime cytotoxic T cells in vivo. *J Exp Med* 192, 1685–1695 (2000).
13. Lei, X. *et al.* CD4+ helper T cells endow cDC1 with cancer-impeding functions in the human tumor micro-environment. *Nat Commun* 14, (2023).
14. Hildner, K. *et al.* Batf3 deficiency reveals a critical role for CD8alpha+ dendritic cells in cytotoxic T cell immunity. *Science* 322, 1097–1100 (2008).
15. Hor, J. L. *et al.* Spatiotemporally Distinct Interactions with Dendritic Cell Subsets Facilitates CD4+ and CD8+ T Cell Activation to Localized Viral Infection. *Immunity* 43, 554–565 (2015).
16. Eickhoff, S. *et al.* Robust Anti-viral Immunity Requires Multiple Distinct T Cell-Dendritic Cell Interactions. *Cell* 162, 1322–1337 (2015).
17. Wu, R. & Murphy, K. M. DCs at the center of help: Origins and evolution of the three-cell-type hypothesis. *J Exp Med* 219, (2022).
18. Wu, R. *et al.* Mechanisms of CD40-dependent cDC1 licensing beyond costimulation. *Nat Immunol* 23, 1536–1550 (2022).
19. Lei, X. *et al.* CD4+ T cells produce IFN-I to license cDC1s for induction of cytotoxic T-cell activity in human tumors. *Cell Mol Immunol* 21, 374–392 (2024).
20. Ridge, J. P., Di Rosa, F. & Matzinger, P. A conditioned dendritic cell can be a temporal bridge between a CD4+ T-helper and a T-killer cell. *Nature* 393, 474–478 (1998).
21. Bennett, S. R. M. *et al.* Help for cytotoxic-T-cell responses is mediated by CD40 signaling. *Nature* 393, 478–480 (1998).
22. Schoenberger, S. P., Toes, R. E. M., Van Dervoort, E. I. H., Offringa, R. & Melief, C. J. M. T-cell help for cytotoxic T lymphocytes is mediated by CD40-CD40L interactions. *Nature* 393, 480–483 (1998).
23. Ahrends, T. *et al.* CD4+ T cell help creates memory CD8+ T cells with innate and help-independent recall capacities. *Nat Commun* 10, (2019).
24. Ahrends, T. *et al.* CD4+ T Cell Help Confers a Cytotoxic T Cell Effector Program Including Coinhibitory Receptor Downregulation and Increased Tissue Invasiveness. *Immunity* 47, 848-861.e5 (2017).

25. Brewitz, A. *et al.* CD8+ T Cells Orchestrate pDC-XCR1+ Dendritic Cell Spatial and Functional Cooperativity to Optimize Priming. *Immunity* 46, 205–219 (2017).

26. Leal, J. M. *et al.* Innate cell microenvironments in lymph nodes shape the generation of T cell responses during type I inflammation. *Sci Immunol* 6, (2021).

27. Nakano, H. *et al.* Blood-derived inflammatory dendritic cells in lymph nodes stimulate acute T helper type 1 immune responses. *Nat Immunol* 10, 394–402 (2009).

28. León, B., López-Bravo, M. & Ardavín, C. Monocyte-derived dendritic cells formed at the infection site control the induction of protective T helper 1 responses against Leishmania. *Immunity* 26, 519–531 (2007).

29. Hohl, T. M. *et al.* Inflammatory monocytes facilitate adaptive CD4 T cell responses during respiratory fungal infection. *Cell Host Microbe* 6, 470–481 (2009).

30. Aldridge, J. R. *et al.* TNF/iNOS-producing dendritic cells are the necessary evil of lethal influenza virus infection. *Proc Natl Acad Sci U S A* 106, 5306–5311 (2009).

31. Ersland, K., Wüthrich, M. & Klein, B. S. Dynamic interplay among monocyte-derived, dermal, and resident lymph node dendritic cells during the generation of vaccine immunity to fungi. *Cell Host Microbe* 7, 474–487 (2010).

32. Goldszmid, R. S. *et al.* NK cell-derived interferon-γ orchestrates cellular dynamics and the differentiation of monocytes into dendritic cells at the site of infection. *Immunity* 36, 1047–1059 (2012).

33. Serbina, N. V. & Pamer, E. G. Monocyte emigration from bone marrow during bacterial infection requires signals mediated by chemokine receptor CCR2. *Nat Immunol* 7, 311–317 (2006).

34. Palframan, R. T. *et al.* Inflammatory chemokine transport and presentation in HEV: a remote control mechanism for monocyte recruitment to lymph nodes in inflamed tissues. *J Exp Med* 194, 1361–1373 (2001).

35. Qu, C. *et al.* Role of CCR8 and other chemokine pathways in the migration of monocyte-derived dendritic cells to lymph nodes. *J Exp Med* 200, 1231–1241 (2004).

36. Samstein, M. *et al.* Essential yet limited role for CCR2+ inflammatory monocytes during Mycobacterium tuberculosis-specific T cell priming. *Elife* 2, (2013).

37. Coillard, A. & Segura, E. Antigen presentation by mouse monocyte-derived cells: Re-evaluating the concept of monocyte-derived dendritic cells. *Mol Immunol* 135, 165–169 (2021).

38. Kuhn, S., Yang, J. & Ronchese, F. Monocyte-Derived Dendritic Cells Are Essential for CD8(+) T Cell Activation and Antitumor Responses After Local Immunotherapy. *Front Immunol* 6, (2015).

39. De Koker, S. *et al.* Inflammatory monocytes regulate Th1 oriented immunity to CpG adjuvanted protein vaccines through production of IL-12. *Sci Rep* 7, (2017).

40. Leirião, P., del Fresno, C. & Ardavín, C. Monocytes as effector cells: activated Ly-6C(high) mouse monocytes migrate to the lymph nodes through the lymph and cross-present antigens to CD8+ T cells. *Eur J Immunol* 42, 2042–2051 (2012).

41. Ersland, K., Wüthrich, M. & Klein, B. S. Dynamic interplay among monocyte-derived, dermal, and resident lymph node dendritic cells during the generation of vaccine immunity to fungi. *Cell Host Microbe* 7, 474–487 (2010).

42. Bosteels, C. *et al.* Inflammatory Type 2 cDCs Acquire Features of cDC1s and Macrophages to Orchestrate Immunity to Respiratory Virus Infection. *Immunity* 52, 1039-1056.e9 (2020).

43. Chow, K. V., Lew, A. M., Sutherland, R. M. & Zhan, Y. Monocyte-Derived Dendritic Cells Promote Th Polarization, whereas Conventional Dendritic Cells Promote Th Proliferation. *J Immunol* 196, 624–636 (2016).

44. Chu, K.-L., Batista, N. V., Girard, M. & Watts, T. H. Monocyte-Derived Cells in Tissue-Resident Memory T Cell Formation. *J Immunol* 204, 477–485 (2020).

45. Ahrends, T. *et al.* CD27 Agonism Plus PD-1 Blockade Recapitulates CD4+ T-cell Help in Therapeutic Anticancer Vaccination. *Cancer Res* 76, 2921–2931 (2016).

46. Babała, N. *et al.* Subcellular Localization of Antigen in Keratinocytes Dictates Delivery of CD4+ T-cell Help for the CTL Response upon Therapeutic DNA Vaccination into the Skin. *Cancer Immunol Res* 6, 835–847 (2018).

47. Alexander, J. *et al.* Development of high potency universal DR-restricted helper epitopes by modification of high affinity DR-blocking peptides. *Immunity* 1, 751–761 (1994).

48. Oosterhuis, K., Aleyd, E., Vrijland, K., Schumacher, T. N. & Haanen, J. B. Rational design of DNA vaccines for the induction of human papillomavirus type 16 E6- and E7-specific cytotoxic T-cell responses. *Hum Gene Ther* 23, 1301–1312 (2012).

49. Hilligan, K. L. *et al.* Dermal IRF4+ dendritic cells and monocytes license CD4+ T helper cells to distinct cytokine profiles. *Nat Commun* 11, (2020).

50. Guilliams, M. *et al.* Unsupervised High-Dimensional Analysis Aligns Dendritic Cells across Tissues and Species. *Immunity* 45, 669–684 (2016).

51. Satpathy, A. T. *et al.* Zbtb46 expression distinguishes classical dendritic cells and their committed progenitors from other immune lineages. *J Exp Med* 209, 1135–1152 (2012).

52. Brühl, H. *et al.* Targeting of Gr-1+,CCR2+ monocytes in collagen-induced arthritis. *Arthritis Rheum* 56, 2975–2985 (2007).

53. Mack, M. *et al.* Expression and characterization of the chemokine receptors CCR2 and CCR5 in mice. *J Immunol* 166, 4697–4704 (2001).

54. Blecher-Gonen, R. *et al.* Single-Cell Analysis of Diverse Pathogen Responses Defines a Molecular Roadmap for Generating Antigen-Specific Immunity. *Cell Syst* 8, 109-121.e6 (2019).

55. Brown, C. C. *et al.* Transcriptional Basis of Mouse and Human Dendritic Cell Heterogeneity. *Cell* 179, 846-863.e24 (2019).

56. Luft, T. *et al.* IFN-alpha enhances CD40 ligand-mediated activation of immature monocyte-derived dendritic cells. *Int Immunol* 14, 367–380 (2002).

57. Schetters, S. T. T. *et al.* Monocyte-derived APCs are central to the response of PD1 checkpoint blockade and provide a therapeutic target for combination therapy. *J Immunother Cancer* 8, (2020).

58. Gressier, E. *et al.* CD4+ T cell calibration of antigen-presenting cells optimizes antiviral CD8+ T cell immunity. *Nat Immunol* 24, 979–990 (2023).

59. Grewal, I. S. & Flavell, R. A. CD40 and CD154 in cell-mediated immunity. *Annu Rev Immunol* 16, 111–135 (1998).

60. Alderson, M. R. *et al.* CD40 expression by human monocytes: regulation by cytokines and activation of monocytes by the ligand for CD40. *J Exp Med* 178, 669–674 (1993).

61. Ruhland, M. K. *et al.* Visualizing Synaptic Transfer of Tumor Antigens among Dendritic Cells. *Cancer Cell* 37, 786-799.e5 (2020).

62. Gurevich, I. *et al.* Active dissemination of cellular antigens by DCs facilitates CD8+ T-cell priming in lymph nodes. *Eur J Immunol* 47, 1802–1818 (2017).

63. Allan, R. S. *et al.* Migratory dendritic cells transfer antigen to a lymph node-resident dendritic cell population for efficient CTL priming. *Immunity* 25, 153–162 (2006).

64. Mondor, I. *et al.* Lymphatic Endothelial Cells Are Essential Components of the Subcapsular Sinus Macrophage Niche. *Immunity* 50, 1453-1466.e4 (2019).

65. Dick, S. A. *et al.* Three tissue resident macrophage subsets coexist across organs with conserved origins and life cycles. *Sci Immunol* 7, (2022).

66. Elewaut, A. *et al.* Cancer cells impair monocyte-mediated T cell stimulation to evade immunity. *Nature* 637, (2025).

67. Flores-Langarica, A. *et al.* T-zone localized monocyte-derived dendritic cells promote Th1 priming to Salmonella. *Eur J Immunol* 41, 2654–2665 (2011).

68. Chaudhri, A. *et al.* PD-L1 Binds to B7-1 Only In Cis on the Same Cell Surface. *Cancer Immunol Res* 6, 921–929 (2018).

69. Zhao, Y. *et al.* PD-L1:CD80 Cis-Heterodimer Triggers the Co-stimulatory Receptor CD28 While Repressing the Inhibitory PD-1 and CTLA-4 Pathways. *Immunity* 51, 1059-1073.e9 (2019).

70. Sugiura, D. *et al.* Restriction of PD-1 function by cis-PD-L1/CD80 interactions is required for optimal T cell responses. *Science* 364, 558–566 (2019).

71. Merad, M., Sathe, P., Helft, J., Miller, J. & Mortha, A. The dendritic cell lineage: ontogeny and function of dendritic cells and their subsets in the steady state and the inflamed setting. *Annu Rev Immunol* 31, 563–604 (2013).

72. De Giovanni, M. *et al.* Spatiotemporal regulation of type I interferon expression determines the antiviral polarization of CD4+ T cells. *Nat Immunol* 21, 321–330 (2020).

73. Lönnberg, T. *et al.* Single-cell RNA-seq and computational analysis using temporal mixture modeling resolves TH1/TFH fate bifurcation in malaria. *Sci Immunol* 2, (2017).

74. Rice, J., Elliott, T., Buchan, S. & Stevenson, F. K. DNA Fusion Vaccine Designed to Induce Cytotoxic T Cell Responses Against Defined Peptide Motifs: Implications for Cancer Vaccines. *The Journal of Immunology* 167, (2001).

Supplementary Information

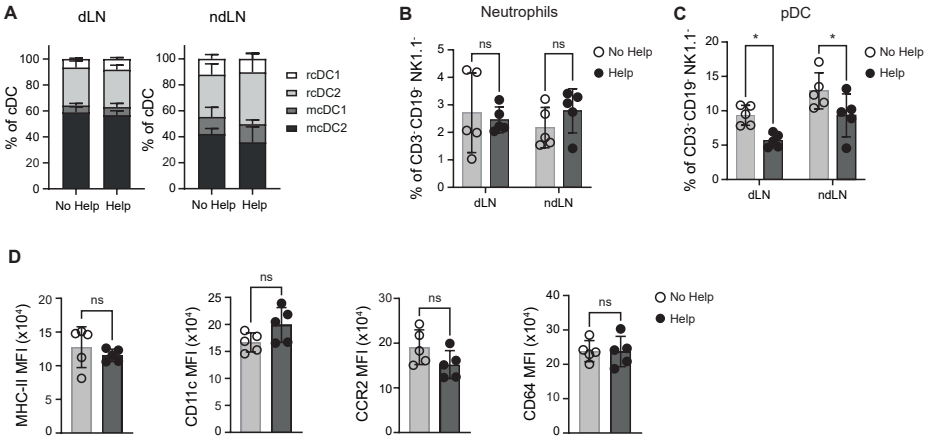

Supplementary Figure 1. Analysis of myeloid cell populations in dLN after Help or No Help vaccination. Mice received Help or No Help vaccine and dLN and ndLN were analyzed by flow cytometry at day 5. **(A)** Frequency of resident ($CD11c^{+}MHC\text{-}II^{int}$) and migratory ($CD11c^{+}MHC\text{-}II^{hi}$) cDC1 ($XCR1^{+}$) and cDC2 ($CD11b^{+}$) within total cDCs. **(B, C)** Quantification of neutrophils (B) and pDCs (C). **(D)** Expression levels of MHC-II, CD11c, CCR2 and CD64 in MFI on MoDC derived from the dLN. Statistics: (A-C) N = 5 mice per group (mean ± SD); Two-way ANOVA with Sidak post hoc test to correct for multiple testing, for comparing Help versus No Help for dLN or ndLN (if not indicated = NS). In panel A the frequency of migDC2 was compared between dLN and ndLN using Two-way ANOVA with Sidak post hoc test to correct for multiple testing. (P=0.0027 in No Help, P=0.0004 in Help); (D) N = 5 mice per group (mean ± SD); Unpaired student's *t*-test. (A-D) Representative of three independently performed experiments.

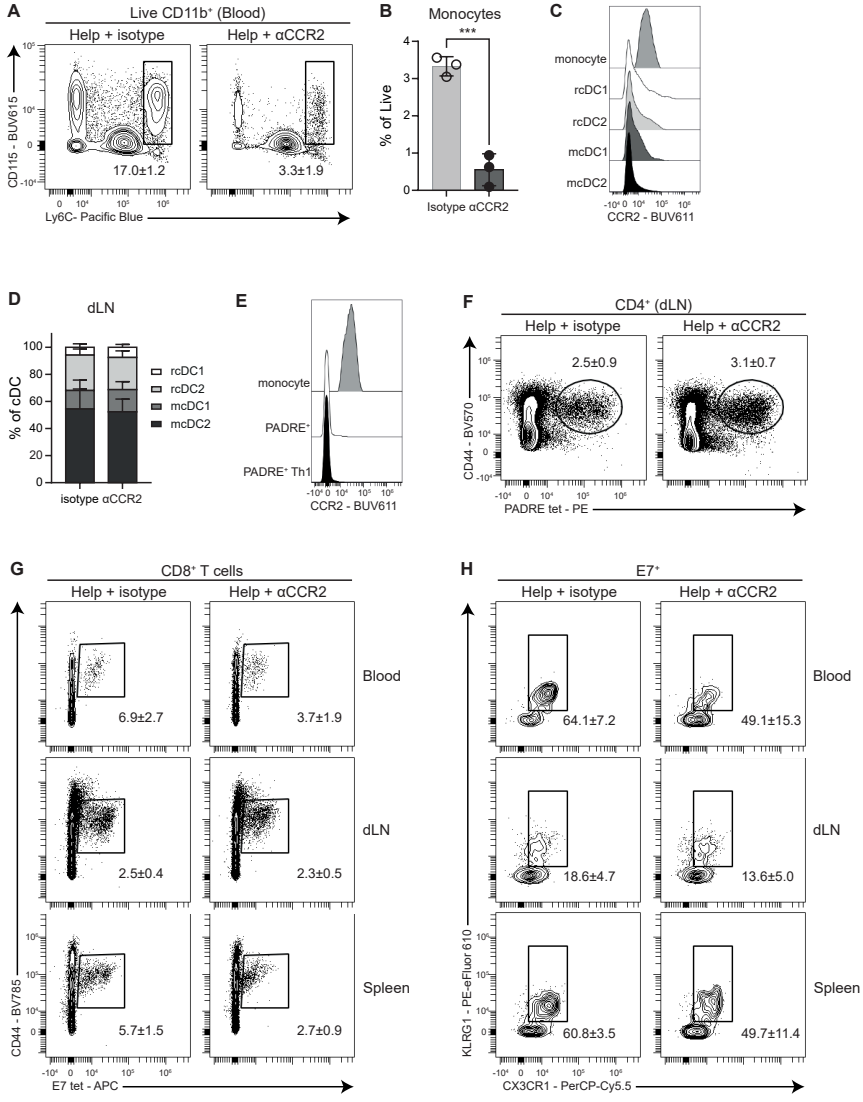

Supplementary Figure 2. MoDCs promote effector differentiation of CD4+ and CD8+ T cells.
(A-B) Representative contour plots (A) and quantification (B) of CD11b+Ly6C+CD115+ monocytes in blood day 4 post antibody injection. Antibodies were administered daily i.p. **(C)** Histograms depicting CCR2 expression by CCR2+Ly6C+CD11b+ monocytes, resident (CD11c+MHC-IIint) and migratory (CD11c+MHC-IIhi) cDC1 (XCR1+) and cDC2 (CD11b+) in the dLN 4 days post vaccination. Data presented are a concatenation of 5 mice. **(D)** Frequency of resident and migratory cDC1 and cDC2 within total cDCs. N=5 mice per group (mean ± SD) **(E)** Histograms depicting CCR2 expression by CCR2+Ly6C+CD11b+ monocytes, CD44+PADRE tet+ CD4+ T cells and Th1 (SLAM+T-bet+) PADRE tet+ in the dLN 4 days post vaccination. Data presented are a concatenation of 5 mice. **(F)** Representative contour plots of PADRE tet+ CD4+ T cells in the dLN d8 post vaccination. **(G-H)** E7 tet+ CD8+ T cells (G) and KLRG1+CX3CR1+E7 tet+ CD8+ T cells (H) in indicated organs. Statistics: (A-B) N = 3 mice per group (mean ± SD), representative of three independently performed experiments; Unpaired student *t*-test. (E, G, H), N = 9 mice per group (mean ± SD) representative of two (C) or three (D-E) independently performed experiments.

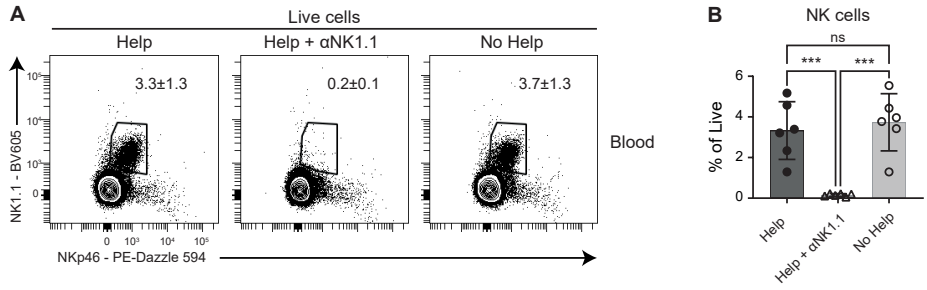

Supplementary Figure 3. Anti-NK1.1 successfully depletes NK cells.
(A-B) Representative contour plots (A) and quantification (B) of $NK1.1^{+}NKp46^{+}$ NK cells in blood day 5 post injection. Antibodies were administered i.p. on day -1, 0 and day 3. Statistics: (A-B) N = 6 mice per group (mean ± SD), representative of one experiment; One-way ANOVA.